



1 **Half-hourly changes in intertidal temperature at nine wave-exposed** 2 **locations along the Atlantic Canadian coast: a 5.5-year study**

3 Ricardo A. Scrosati, Julius A. Ellrich, Matthew J. Freeman

4 Department of Biology, St. Francis Xavier University, Antigonish, Nova Scotia B2G 2W5, Canada

5 *Correspondence to:* Ricardo A. Scrosati (rscrosat@stfx.ca)

6 **Abstract.** Intertidal habitats are unique because they spend alternating periods of
7 submergence (at high tide) and emergence (at low tide) every day. Thus, intertidal temperature
8 is mainly driven by sea surface temperature (SST) during high tides and by air temperature
9 during low tides. Because of that, the switch from high to low tides and viceversa can determine
10 rapid changes in intertidal thermal conditions. On cold-temperate shores, which are
11 characterized by cold winters and warm summers, intertidal thermal conditions can also change
12 considerably with seasons. Despite this uniqueness, knowledge on intertidal temperature
13 dynamics is more limited than for open seas. This is especially true for wave-exposed intertidal
14 habitats, which, in addition to the unique properties described above, are also characterized by
15 wave splash being able to moderate intertidal thermal extremes during low tides. To address this
16 knowledge gap, we measured temperature every half hour during a period of 5.5 years (2014–
17 2019) at nine wave-exposed rocky intertidal locations along the Atlantic coast of Nova Scotia,
18 Canada. This data set is freely available from the figshare online repository (Scrosati and
19 Ellrich, 2020a; <https://doi.org/10.6084/m9.figshare.12462065.v1>). We summarize the main
20 properties of this data set by focusing on location-wise values of daily maximum and minimum
21 temperature and daily SST, which we make freely available as a separate data set in figshare
22 (Scrosati et al., 2020; <https://doi.org/10.6084/m9.figshare.12453374.v1>). Overall, this cold-
23 temperate coast exhibited a wide annual SST range, from a lowest overall value of $-1.8\text{ }^{\circ}\text{C}$ in
24 winter to a highest overall value of $22.8\text{ }^{\circ}\text{C}$ in summer. In addition, the latitudinal SST trend
25 along this coast experienced a reversal from winter, when SST increased southwards, to
26 summer, when SST decreased southwards, seemingly driven by alongshore differences in
27 coastal upwelling. Daily temperature maxima and minima were more extreme, as expected from
28 their occurrence during low tides, ranging from a lowest overall value of $-16.3\text{ }^{\circ}\text{C}$ in winter to a
29 highest overall value of $41.2\text{ }^{\circ}\text{C}$ in summer. Daily maximum temperature in summer varied little
30 along the coast, while daily minimum temperature in winter increased southwards. This data set
31 is the first of its kind for the Atlantic Canadian coast and exemplifies in detail how intertidal
32 temperature varies in wave-exposed environments on a cold-temperate coast.

33 **1 Introduction**

34 Rocky intertidal habitats occur on marine rocky shores between the highest and lowest
35 elevations reached by tides. These environments are unique because they spend alternating
36 periods of submergence (during high tides) and emergence (during low tides) every day
37 (Raffaelli and Hawkins, 1999; Menge and Branch, 2001). Thus, on the one hand, intertidal
38 conditions are influenced by the seasonal changes in sea surface temperature (SST), which can
39 be pronounced on temperate shores, which display warm waters in summer but cold waters in
40 winter. On the other hand, an even greater degree of thermal variation can occur at hourly scales



41 once intertidal habitats become exposed to the air at low tide, especially on hot days in spring
42 and summer (Watt and Scrosati, 2013; Lathlean et al., 2014; Umanzor et al., 2017) and cold
43 days in winter (Scrosati and Ellrich, 2018a).

44 Temperature is a major factor influencing the distribution and abundance of species
45 (Pörtner, 2002; Körner et al., 2016; Lancaster and Humphreys, 2020). Thus, SST plays an
46 important ecological role in intertidal habitats during high tides (Sanford, 2014), while high
47 (Somero 2007) and low (Braby 2007) air temperatures are ecologically relevant during low
48 tides. In addition, not only average temperature matters, but its temporal variability as well
49 (Benedetti-Cecchi et al., 2006). Overall, then, having detailed temperature data across periods
50 of low and high tide is important for intertidal ecology and to make biogeographic predictions
51 based on climate change expectations (Wetthey et al., 2011).

52 Temperature data are available for surface ocean waters worldwide (Fay and McKinley,
53 2014; Banzon et al., 2016; Freeman and Lovenduski, 2016; Aulicino et al., 2018; Yun et al.,
54 2019). However, data on intertidal temperature are considerably less common, both in terms of
55 spatial and temporal coverage (Lathlean et al., 2014; Umanzor et al., 2017; Scrosati and Ellrich,
56 2018a). This is especially true for wave-exposed intertidal habitats, as remote sensing methods
57 that are commonly used for open waters (e.g., satellites) cannot capture the quick, localized
58 temperature changes caused by tides and waves on exposed shores. Waves can also damage
59 equipment deployed in-situ to measure intertidal temperature. For wave-exposed intertidal
60 habitats, temperature data between consecutive low and high tides can also be used to infer
61 physical aspects of the environment such as wave action itself (Harley and Helmuth, 2003).

62 Wave-exposed rocky intertidal habitats are common along the Atlantic Canadian coast in
63 Nova Scotia, as this coast faces the open ocean. Several studies have investigated the ecology of
64 these environments (Minchinton and Scheibling, 1991; Hunt and Scheibling, 1998, 2001;
65 Scrosati and Heaven, 2007; Arribas et al., 2014; Molis et al., 2015; Ellrich and Scrosati, 2016;
66 Scrosati and Ellrich, 2018b, 2019; Scrosati, 2020). However, because of their research goals,
67 intertidal temperature was either not measured or analyzed for a few locations or limited time
68 periods. Therefore, there is a knowledge gap on broad spatio-temporal patterns in intertidal
69 temperature for wave-exposed environments along this coast. To address this gap, in this article
70 we provide and discuss a data set consisting of intertidal temperature values measured every half
71 hour at nine wave-exposed locations along the Atlantic coast of Nova Scotia spanning a period
72 of 5.5 years.

73 **2 Methods**

74 We monitored intertidal temperature at nine locations that span the full extent of the open
75 Atlantic coast of mainland Nova Scotia, nearly 415 km (Fig. 1). For simplicity, these locations
76 will hereafter be referred to as L1 to L9, from north to south. Their names and coordinates are
77 provided in Table 1. The substrate of these intertidal locations is stable bedrock. All of them
78 face the open Atlantic Ocean without physical obstructions, so they are wave-exposed. Values
79 of daily maximum water velocity (an indication of wave exposure) measured with
80 dynamometers (see design in Bell and Denny, 1994) in wave-exposed intertidal habitats from
81 this coast range between 6–12 m s⁻¹ (Hunt and Scheibling, 2001; Scrosati and Heaven, 2007;
82 Ellrich and Scrosati, 2017).



83 We started to monitor intertidal temperature in April-May 2014 at L2-L9 and in April 2015
84 at L1 (see the precise dates in Scrosati and Ellrich, 2020a). We measured temperature with
85 submersible loggers (HOBO Pendant logger, Onset Computer, Bourne, MA, USA) that were
86 kept attached to the intertidal substrate with plastic cable ties secured to eye screws drilled into
87 the substrate, allowing almost no contact between the loggers and the substrate. We kept the
88 substrate around the loggers always free of macroalgal canopies and sessile invertebrates. To
89 have a continuous temperature record during the 5.5 years of this study, we replaced the loggers
90 periodically. At each location, we installed replicate loggers several meters apart from one
91 another at an elevation just above the mid-intertidal zone. We set the loggers to record
92 temperature every 30 min. We stopped recording temperature in November 2018 at L1 and L3
93 and in August-October 2019 at L2 and L4-L9 (see the precise dates in Scrosati and Ellrich,
94 2020a). For each location, temperature was highly correlated between the replicate loggers
95 during the study period (mean $r = 0.97$). Thus, we averaged the corresponding half-hourly
96 values to generate one time series of half-hourly temperature data for each location for the
97 studied period, which is the data set on which this paper is based (Scrosati and Ellrich, 2020a).

98 Due to its high temporal resolution, this data set could be used in the future for a variety of
99 purposes. To summarize its main properties here, we extracted values that are commonly used in
100 intertidal ecology and coastal oceanography and that therefore could be of immediate interest:
101 daily maximum and minimum temperature (MaxT and MinT, respectively) and daily SST. As
102 the Nova Scotia coast is cold-temperate, we expected SST to be often considerably lower than
103 MaxT in spring and summer, as MaxT is then reached during low tides when intertidal
104 environments are usually exposed to high air temperatures. Conversely, we expected SST and
105 MaxT to be more similar or even the same in winter, as low tides then often expose intertidal
106 habitats to negative air temperatures below the freezing point of seawater. For these same
107 reasons, we also expected SST to be typically higher than MinT in winter, as MinT is then
108 generally reached during low tides, but more similar to MinT in spring and summer. For each
109 location, we extracted the values of daily MaxT, MinT, and SST from the corresponding set of
110 half-hourly data on intertidal temperature (Scrosati and Ellrich, 2020a). We considered daily
111 SST as the temperature recorded closest to the time of the highest tide of each day, as the
112 loggers were then fully submerged in seawater. We determined the time of such tides using
113 information (Tide and Current Predictor, 2020) for the tide reference stations that are closest to
114 our intertidal locations (Table 1).

115 **3 Main patterns in the data and relevance to future research**

116 We obtained half-hourly temperature data during the monitoring period specified above for
117 each location with just two exceptions: the period between 20 March and 12 April 2017 for L1
118 because of logger removal by drift sea ice coming from the Gulf of St. Lawrence and the period
119 between 30 September 2014 and 26 April 2015 for L9 because of logger loss caused by wave
120 action. Continued monitoring after both such periods was possible after installing new loggers.
121 This data set is available online (Scrosati and Ellrich, 2020a).

122 The temporal changes in daily MaxT, MinT, and SST during the studied period at each
123 location are shown in Fig. 2. For convenience, all of these daily values are also available from
124 the figshare online repository (Scrosati et al., 2020). The highest and lowest values of SST for
125 each location (Table 2) reveal that this cold-temperate coast has a wide seasonal range of SST
126 (see worldwide SST ranges in figure 6.3 in Stewart, 2008). The highest location-wise values of



127 SST occurred in summer and ranged between 20 °C and 22.8 °C, while the lowest location-wise
128 SST values occurred in winter and were near the freezing point of seawater, between -0.9 °C
129 and -1.8 °C (Table 2, Fig. 2). We note that, unlike the nearby Gulf of St. Lawrence (Fig. 1;
130 Saucier et al., 2003) or wave-sheltered coves along the Atlantic coast of Nova Scotia, open
131 waters washing wave-exposed habitats along the Atlantic coast of Nova Scotia do not freeze in
132 winter (Canadian Ice Service, 2020). Overall, for the studied period, the location-wise difference
133 between the highest and lowest SST values ranged between 21.1 °C and 24.6 °C. Although there
134 was some patchiness in this seasonal SST range along the coast, it was lowest in two southern
135 locations (L7 and L9) driven by lower values of maximum summer SST there (Table 2).

136 The occurrence of the lowest location-wise values of maximum summer SST at two
137 southern locations (L7 and L9) is related to a broader alongshore pattern. Based on the data for
138 the summer months (for convenience, July, August, and September) for the years when SST was
139 measured at all locations in those months (2015, 2016, 2017, and 2018), mean location-wise
140 SST in summer decreased from north to south, from 17.5 °C at L1 to 13.2 °C at L9 (Table 2). In
141 contrast, an equivalent analysis done for winter months (for convenience, January, February,
142 and March) for the years when SST was measured at all locations in those months (2016, 2017,
143 and 2018) revealed that mean location-wise SST in winter actually increased from north to
144 south, from 0.8 °C at L1 to 3.0 °C at L9 (Table 2). In other words, a summer-to-winter reversal
145 in the latitudinal trend in intertidal SST takes place on this coast, as waters are warmer in
146 summer and colder in winter in northern locations than in southern locations.

147 The southward decrease of intertidal SST in summer is likely influenced by alongshore
148 differences in coastal upwelling. On the Atlantic coast of Nova Scotia, upwelling-favourable
149 winds are more common in summer than in winter (Garrett and Loucks, 1976; Dever et al.,
150 2018). Although possible alongshore differences in upwelling have not been studied in detail,
151 they seem to exist. For example, Petrie et al. (1987) reported that seawater temperature at 6-20
152 m of depth decreased from June to July 1984 near L6–L7 because of wind-driven upwelling,
153 while temperature at those depths increased north of that coastal range during that period. More
154 recently, Shan et al. (2016) have also referred to wind-driven upwelling on the southeastern
155 Nova Scotia coast. A detailed analysis of daily changes in intertidal SST is beyond the
156 objectives of this data paper. However, Fig. 2 reveals basic differences in summer cooling
157 between northern and southern locations. Summer cooling events were generally marked in
158 southern locations, especially at L6 and L7, where SST could drop by 10 °C in 5-10 days, in
159 some cases reaching values below 5 °C (Fig. 2). An analysis of coastal winds at L6 and L7
160 indicated that wind-driven upwelling explained the cooling observed at those locations in July
161 2014 (Scrosati and Ellrich, 2020b). Although persistent, the summer cooling signal that was
162 often pronounced at L6 and L7 (Fig. 2) weakened progressively towards northern locations,
163 especially at L1 and L2. In fact, at L1, SST never dropped below 10 °C in summer months (Fig.
164 2). These considerations could orient future research to unravel the drivers of the latitudinal
165 changes in summer SST revealed by this study.

166 The southward increase of intertidal SST observed in winter could be a result of latitudinal
167 changes in heat flux from the atmosphere (Stewart, 2008; Deser et al., 2010; Shan et al., 2016),
168 although other processes are also generally at play in coastal environments (Hebert et al., 2016;
169 Larouche and Galbraith, 2016). For example, for the studied coast, the abundant sea ice formed
170 across the Gulf of St. Lawrence (Fig. 1) every winter (Saucier et al., 2003) may contribute to
171 keep intertidal SST low at our northern locations, as the waters that leave this gulf flow



172 southwards following the coast of mainland Nova Scotia (Han et al., 1997; Hebert et al., 2016;
173 Dever et al., 2018), reaching our northern locations first before they warm up on their way
174 south.

175 As expected from the warm summers and cold winters that characterize eastern Canada
176 (Government of Canada, 2020), MaxT was often considerably higher than SST in spring and
177 summer and MinT was often lower than SST in fall and winter (Fig. 2), as MaxT and MinT
178 typically take place at low tide during those respective seasons. The highest location-wise values
179 of MaxT almost doubled those of SST, as they ranged between 36.1°C and 41.2 °C. The lowest
180 location-wise values of MinT ranged between -9.1 °C and -16.3 °C. Therefore, the location-wise
181 difference between the highest and lowest daily temperatures, which ranged between 46.1 °C
182 and 54.4 °C, generally more than doubled the location-wise difference between the highest and
183 lowest daily SST values (Table 2).

184 The highest value of MaxT differed little among locations (Table 2). Based on the data for
185 the summer months (for convenience, July, August, and September) for the years when SST was
186 measured at all locations in those months (2015, 2016, 2017, and 2018), mean location-wise
187 MaxT in summer exhibited patchiness along the coast without any clear latitudinal trend (Table
188 2). As MaxT in summer generally occurs during aerial exposure at low tides, both climatic and
189 oceanographic influences may interact to determine its alongshore pattern. For instance, summer
190 values of MaxT might simply be expected to increase southwards following warmer air
191 temperatures on land (Government of Canada, 2020). However, the SST drops due to coastal
192 upwelling in southern locations in summer might actually temper air temperatures right on the
193 coast, thus limiting MaxT. In the end, climate and oceanography might together be responsible
194 for the patchy alongshore MaxT pattern, which seems dependent on local conditions.
195 Researching these possibilities could thus be of interest. In contrast, the data for winter months
196 (for convenience, January, February, and March) for the years when MinT was measured at all
197 locations in those months (2016, 2017, and 2018) revealed that mean location-wise MinT in
198 winter generally increased from north to south, the lowest such average (-2.7 °C) registered at
199 L1 and the highest one (0.2 °C) at L9 (Table 2). Thus, the alongshore pattern of winter MinT
200 may more clearly respond to typical latitudinal changes in winter air temperatures and perhaps
201 also to influences of Gulf of St. Lawrence sea ice (see above) on northern locations.

202 Another salient property of our data is that the daily changes in MaxT in spring and
203 summer and MinT in fall and winter were much larger than the corresponding daily changes in
204 SST (Fig. 2). Such a high day-to-day variability in MaxT and MinT likely reflects daily changes
205 in weather conditions, which affect intertidal habitats at low tides, as well as wave exposure, as
206 wave-generated splash during low tides on wavy days keep intertidal habitats wet and, thus,
207 often cooler than the air in summer and warmer than the air in winter. Thus, the interaction
208 between weather and wave action as a determinant of intertidal thermal extremes is another
209 research area deserving attention in the future. Ultimately, given the prominent role of extreme
210 abiotic events in ecology (Denny et al., 2009; Smith, 2011; Nowicki et al., 2019), the marked
211 daily changes in MaxT and MinT during those seasons highlight the potentially critical role of
212 low tides for the survival of intertidal organisms on these environmentally variable habitats.

213 Another interesting characteristic of our data set is that the daily average between MaxT
214 and MinT was generally higher than SST in spring and summer but generally lower than SST in
215 fall and winter (Fig. 2). In other words, the average intertidal temperature measured during low
216 tides increased faster from winter to summer and decreased faster from summer to winter than



217 SST. This difference likely reflects the difference in heat capacity between air and water, which
218 makes SST follow air temperatures throughout seasons with a delay (Stewart, 2008).

219 Our data set could also be useful to investigate climatic drivers of interannual differences in
220 intertidal temperature. For example, a marked difference in upwelling-driven coastal cooling at
221 L6 and L7 between July 2014 (strong) and July 2015 (weak) was related to a normal (2014)
222 versus El Niño (2015) conditions (Scrosati and Ellrich, 2020b). Although El Niño (ENSO) is
223 predominantly a Pacific phenomenon (Timmermann et al., 2018), it is also related to interannual
224 weather changes in North America through climatic teleconnections (George and Wolfe 2009;
225 Wu and Lin 2012; Whan and Zwiers 2017; Dai and Tan, 2019). Another large-scale climate
226 phenomenon, the North Atlantic Oscillation (NAO), influences weather patterns mainly in the
227 North Atlantic basin (Hanna and Cropper, 2017). It would thus be interesting to study whether
228 NAO and ENSO might interact (Wu and Lin, 2012; Nalley et al., 2019) to affect winds,
229 upwelling, and ultimately intertidal temperature along the Nova Scotia coast.

230 **4 Conclusions**

231 This is a unique data set because it describes intertidal temperature with a high temporal
232 resolution during a period of 5.5 years at nine wave-exposed locations spanning the full extent
233 of the Atlantic coast of mainland Nova Scotia. The main patterns described above have revealed
234 previously unknown latitudinal and seasonal trends in intertidal temperature on this coast. The
235 considerations on the possible mechanisms underlying these patterns should help orient future
236 research on the drivers of thermal variation in these intertidal environments. Because of the
237 temporal and spatial scales of this data set, we believe that future research using these data could
238 lead to theoretical advances in coastal oceanography and intertidal thermal ecology. Ultimately,
239 this data set represents a detailed baseline on which to study the influence of climatic and
240 oceanographic change on intertidal temperature variation in this cold-temperate system.

241 **Data availability**

242 The full data set on half-hourly temperature measured at the nine intertidal locations
243 between 2014 and 2019 is available from the figshare online repository (Scrosati and Ellrich,
244 2020a; <https://doi.org/10.6084/m9.figshare.12462065.v1>). The daily values of MaxT, MinT, and
245 SST for these locations during this time period are also available from the figshare online
246 repository (Scrosati et al., 2020; <https://doi.org/10.6084/m9.figshare.12453374.v1>).

247 **Author contributions**

248 RAS designed the study. RAS and JAE led field work and JAE and MJF data curation.
249 RAS wrote the manuscript and JAE and MJF reviewed it before submission.

250 **Competing interests**

251 The authors declare that they have no conflict of interest.

252 **Acknowledgements**

253 We thank Alexis Catalán, Carmen Denfeld, Willy Petzold, and Maike Willers for field
254 assistance.

255



255 **Financial support**

256 This study was funded by grants awarded to RAS by the Natural Sciences and Engineering
257 Research Council of Canada (NSERC Discovery Grant #311624), the Canada Research Chairs
258 program (CRC grant #210283), and the Canada Foundation for Innovation (CFI Leaders
259 Opportunity Grant #202034) and by a postdoctoral fellowship awarded to JAE by the German
260 Academic Exchange Service (DAAD fellowship #91617093).

261 **References**

- 262 Arribas, L. P., Donnarumma, L., Palomo, M. G., and Scrosati, R. A.: Intertidal mussels as
263 ecosystem engineers: their associated invertebrate biodiversity under contrasting wave
264 exposures, *Mar. Biodiv.*, 44, 203–211, 2014.
- 265 Aulicino, G., Cotroneo, Y., Ansorge, I., van den Berg, M., Cesarano, C., Belmonte Rivas, M.,
266 and Olmedo Casal, E.: Sea surface salinity and temperature in the southern Atlantic Ocean
267 from South African icebreakers, 2010–2017, *Earth Syst. Sci. Data*, 10, 1227–1236, 2018.
- 268 Banzon, V., Smith, T. M., Chin, T. M., Liu, C., and Hankins, W.: A long-term record of blended
269 satellite and in-situ sea surface temperature for climate monitoring, modeling, and
270 environmental studies, *Earth Syst. Sci. Data*, 8, 165–176, 2016.
- 271 Bell, E. C., and Denny, M. W.: Quantifying "wave exposure": a simple device for recording
272 maximum velocity and results of its use at several field sites, *J. Exp. Mar. Biol. Ecol.*, 181, 9–
273 29, 1994.
- 274 Bennedetti-Cecchi, L., Bertocci, I., Vaselli, S., and Maggi, E.: Temporal variance reverses the
275 impact of high mean intensity of stress in climate change experiments, *Ecology*, 87, 2489–
276 2499, 2006.
- 277 Braby, C. E.: Cold stress, in: *Encyclopedia of Tidepools and Rocky Shores*, edited by: Denny,
278 M. W., and Gaines, S. D., University of California Press, Berkeley, 148–150, 2007.
- 279 Canadian Ice Service: Ice forecasts and observations, [https://www.canada.ca/en/environment-
280 climate-change/services/ice-forecasts-observations.html](https://www.canada.ca/en/environment-climate-change/services/ice-forecasts-observations.html), 2020.
- 281 Dai, Y., and Tan, B.: On the role of the Eastern Pacific teleconnection in ENSO impacts on
282 wintertime weather over East Asia and North America. *J. Clim.*, 32, 1217–1234, 2019.
- 283 Denny, M. W., Hunt, L. J. H., Miller, L. P., and Harley, C. D. G.: On the prediction of extreme
284 ecological events. *Ecol. Monogr.*, 79, 397–421, 2009.
- 285 Deser, C., Alexander, M. A., Xie, S. P., and Phillips, A. S.: Sea surface temperature variability:
286 patterns and mechanisms, *Annu. Rev. Mar. Sci.*, 2, 115–143, 2010.
- 287 Dever, M., Skagseth, Ø., Drinkwater, K., and Hebert, D.: Frontal dynamics of a buoyancy-
288 driven coastal current: quantifying buoyancy, wind, and isopycnal tilting influence on the
289 Nova Scotia current, *J. Geophys. Res. Oceans*, 123, 4988–5003, 2018.
- 290 Ellrich, J. A., and Scrosati, R. A.: Water motion modulates predator nonconsumptive limitation
291 of prey recruitment, *Ecosphere*, 7, e01402, 2016.



- 292 Ellrich, J. A., and Scrosati, R. A.: Maximum water velocities in wave-exposed rocky intertidal
293 habitats from Deming Island, Atlantic coast of Nova Scotia, Canada, Pangaea data set,
294 <https://doi.pangaea.de/10.1594/pangaea.880722>, 2017.
- 295 Fay, A. R., and McKinley, G. A.: Global open-ocean biomes: mean and temporal variability,
296 *Earth Syst. Sci. Data*, 6, 273–284, 2014.
- 297 Freeman, N. M., and Lovenduski, N. S.: Mapping the Antarctic Polar Front: weekly realizations
298 from 2002 to 2014, *Earth Syst. Sci. Data*, 8, 191–198, 2016.
- 299 Garrett, C. J. R., and Loucks, R. H.: Upwelling along the Yarmouth shore of Nova Scotia, J.
300 *Fish. Res. Board Can.*, 33, 116–117, 1976.
- 301 George, S. S., and Wolfe, S.A.: El Niño stills winter winds across the southern Canadian
302 Prairies, *Geophys. Res. Lett.*, 36, L23806, 2009.
- 303 Government of Canada: Past weather and climate, Historical data,
304 http://climate.weather.gc.ca/historical_data/search_historic_data_e.html, 2020.
- 305 Han, G., Hannah, C. G., Loder, J. W., and Smith, P. C.: Seasonal variation of the three-
306 dimensional mean circulation over the Scotian Shelf, *J. Geophys. Res.*, 102, 1011–1025, 1997.
- 307 Hanna, E., and Cropper, T. E.: North Atlantic Oscillation, Oxford Research Encyclopedia of
308 Climate Science, Oxford University Press,
309 <http://doi.org/10.1093/acrefore/9780190228620.013.22>, 2017.
- 310 Harley, C. D. G., and Helmuth, B. S. T.: Local- and regional-scale effects of wave exposure,
311 thermal stress, and absolute versus effective shore level on patterns of intertidal zonation,
312 *Limnol. Oceanogr.*, 48, 1498–1508, 2003.
- 313 Hebert, D., Pettipas, R., Brickman, D., and Dever, M.: Meteorological, sea ice, and physical
314 oceanographic conditions on the Scotian Shelf and in the Gulf of Maine during 2015, DFO
315 *Can. Sci. Advis. Sec. Res. Doc.* 2016/083, 2016.
- 316 Hunt, H. L., and Scheibling, R. E.: Effects of whelk (*Nucella lapillus* (L.)) predation on mussel
317 (*Mytilus trossulus* (Gould), *M. edulis* (L.)) assemblages in tidepools and on emergent rock on a
318 wave-exposed rocky shore in Nova Scotia, Canada, *J. Exp. Mar. Biol. Ecol.*, 226, 87–113,
319 1998.
- 320 Hunt, H. L., and Scheibling, R. E.: Patch dynamics of mussels on rocky shores: integrating
321 process to understand pattern, *Ecology*, 82, 3213–3231, 2001.
- 322 Körner, C., Basler, D., Hoch, G., Kollas, C., Lenz, A., Randin, C. F., Vitasse, Y., and
323 Zimmermann, N.E.: Where, why and how? Explaining the low-temperature range limits of
324 temperate tree species, *J. Ecol.*, 104, 1076–1088, 2016.
- 325 Lancaster, L. T., and Humphreys, A. M.: Global variation in the thermal tolerances of plants,
326 *Proc. Nat. Acad. Sci. U. S. A.*, 117, 13580–13587, 2020.
- 327 Larouche, P., and Galbraith, P. S.: Canadian coastal seas and Great Lakes sea surface
328 temperature climatology and recent trends, *Can. J. Remote Sens.*, 42, 243–258, 2016.
- 329 Lathlean, J. A., Ayre, D. J., and Minchinton, T. E.: Estimating latitudinal variability in extreme
330 heat stress on rocky intertidal shores, *J. Biogeogr.*, 41, 1478–1491, 2014.



- 331 Menge, B. A., and Branch, G. M.: Rocky intertidal communities, in: *Marine Community*
332 *Ecology*, edited by: Bertness, M. D., Gaines, S. D., and Hay, M. H., Sinauer, Sunderland, 221–
333 251, 2001.
- 334 Minchinton, T. E., and Scheibling, R. E.: The influence of larval supply and settlement on the
335 population structure of barnacles, *Ecology*, 72, 1867–1879, 1991.
- 336 Molis, M., Scrosati, R. A., El-Belely, E. F., Lesniowski, T., and Wahl, M.: Wave-induced
337 changes in seaweed toughness entail plastic modifications in snail traits maintaining
338 consumption efficacy, *J. Ecol.*, 103, 851–859, 2015.
- 339 Nalley, D., Adamowski, J., Biswas, A., Gharabaghi, B., and Hu, W.: A multiscale and
340 multivariate analysis of precipitation and streamflow variability in relation to ENSO, NAO,
341 and PDO, *J. Hydrol.*, 574, 288–307, 2019.
- 342 Nowicki, R., Heithaus, M., Thomson, J., Burkholder, D., Gastrich, K., and Wirsing, A.: Indirect
343 legacy effects of an extreme climatic event on a marine megafaunal community, *Ecol.*
344 *Monogr.*, 89, article e01365, 2019.
- 345 Petrie, B., Topliss, B. J., and Wright, D. G.: Coastal upwelling and eddy development off Nova
346 Scotia, *J. Geophys. Res.*, 29, 12979–12991, 1987.
- 347 Pörtner, H. O.: Climate variations and the physiological basis of temperature-dependent
348 biogeography: systemic to molecular hierarchy of thermal tolerance in animals, *Comp.*
349 *Biochem. Physiol. Part A: Mol. Integr. Physiol.*, 132, 739–761, 2002.
- 350 Raffaelli, D., and Hawkins, S.: *Intertidal Ecology*, Chapman & Hall, London, 1999.
- 351 Sanford, E.: The biogeography of marine communities, in: *Marine Community Ecology and*
352 *Conservation*, edited by: Bertness, M. D., Bruno, J. F., Silliman, B. R., and Stachowicz, J. J.,
353 Sinauer, Sunderland, 131–163, 2014.
- 354 Saucier, F. J., Roy, F., Gilbert, D., Pellerin, P., and Ritchie, H.: Modeling the formation and
355 circulation processes of water masses and sea ice in the Gulf of St. Lawrence, Canada, *J.*
356 *Geophys. Res.*, 108, article 3269, 2003.
- 357 Scrosati, R. A.: Upwelling spike and marked SST drop after the arrival of cyclone Dorian to the
358 Atlantic Canadian coast, *J. Sea Res.*, 159, article 101888, 2020.
- 359 Scrosati, R. A., and Ellrich, J. A.: Thermal moderation of the intertidal zone by seaweed
360 canopies in winter, *Mar. Biol.*, 165: article 115, 2018a.
- 361 Scrosati, R. A., and Ellrich, J. A.: Benthic-pelagic coupling and bottom-up forcing in rocky
362 intertidal communities along the Atlantic Canadian coast, *Ecosphere*, 9, e02229, 2018b.
- 363 Scrosati, R. A., and Ellrich, J. A.: A 5-year study (2014–2018) of the relationship between
364 coastal phytoplankton abundance and intertidal barnacle size along the Atlantic Canadian
365 coast, *PeerJ*, 7, article e6892, 2019.
- 366 Scrosati, R. A., and Ellrich, J. A.: Half-hourly temperature data measured at nine wave-exposed
367 intertidal locations along the Atlantic coast of Nova Scotia, Canada (2014–2019), figshare data
368 set, <https://doi.org/10.6084/m9.figshare.12462065.v1>, 2020a.



- 369 Scrosati, R. A., and Ellrich, J. A.: Marked contrast in wind-driven upwelling on the southeastern
370 Nova Scotia coast in July of two years differing in ENSO conditions, *Oceanol. Hydrobiol.*
371 *Stud.*, 49, 81–87, 2020b.
- 372 Scrosati, R. A., Ellrich, J. A., and Freeman, M. J.: Daily SST, maximum temperature, and
373 minimum temperature at nine wave-exposed intertidal locations along the Atlantic coast of
374 Nova Scotia, Canada (2014–2019), figshare data set,
375 <https://doi.org/10.6084/m9.figshare.12453374.v1>, 2020.
- 376 Scrosati, R., and Heaven, C.: Spatial trends in community richness, diversity, and evenness
377 across rocky intertidal environmental stress gradients in eastern Canada, *Mar. Ecol. Prog. Ser.*,
378 342, 1–14, 2007.
- 379 Shan, S., Sheng, J., Ohashi, K., and Dever, M.: Assessing the performance of a multi-nested
380 ocean circulation model using satellite remote sensing and in-situ observations, *Satell.*
381 *Oceanogr. Meteorol.*, 1, 39–59, 2016.
- 382 Smith, M. D.: An ecological perspective on extreme climatic events: a synthetic definition and
383 framework to guide future research, *J. Ecol.*, 99, 656–663, 2011.
- 384 Somero, G.: Heat stress, in: *Encyclopedia of Tidepools and Rocky Shores*, edited by: Denny, M.
385 W., and Gaines, S. D., University of California Press, Berkeley, 266–270, 2007.
- 386 Stewart, R. H.: Introduction to physical oceanography, Open Textbook Library,
387 <https://open.umn.edu/opentextbooks/bookdetail.aspx?bookid=20>, 2008.
- 388 Tide and Current Predictor: Tidal height and current site selection,
389 <http://tbone.biol.sc.edu/tide/index.html>, 2020.
- 390 Timmermann, A., An, S., Kug, J. S., Jin, F. F., Cai, W., Capotondi, A., Cobb, K., Lengaigne,
391 M., McPhaden, M. J., Stuecker, M. F., Stein, K., Wittenberg, A. T., Yun, K. S., Bayr, T.,
392 Chen, H. C., Chikamoto, Y., Dewitte, B., Dommenges, D., Grothe, P., Guilyardi, E., Ham, Y.
393 G., Hayashi, M., Ineson, S., Kang, D., Kim, S., Kim, W., Lee, J. Y., Li, T., Luo, J. J.,
394 McGregor, S., Planton, Y., Power, S., Rashid, H., Ren, H. L., Santoso, A., Takahashi, K.,
395 Todd, A., Wang, G., Wang, G., Xie, R., Yang, W. H., Yeh, S. W., Yoon, J., Zeller, E., and
396 Zhang, X.: El Niño–Southern Oscillation complexity, *Nature*, 559, 535–545, 2018.
- 397 Umazor, S., Ladah, L., Calderón-Aguilera, L. E., and Zertuche-González, J. A.: Intertidal
398 macroalgae influence macroinvertebrate distribution across stress scenarios, *Mar. Ecol. Prog.*
399 *Ser.*, 584, 67–77, 2017.
- 400 Watt, C. A., and Scrosati, R. A.: Bioengineer effects on understory species richness, diversity,
401 and composition change along an environmental stress gradient: experimental and mensurative
402 evidence, *Estuar. Coast. Shelf Sci.*, 123, 10–18, 2013.
- 403 Wethey, D. S., Woodin, S. A., Hilbish, T. J., Jones, S. J., Lima, F. P., and Brannock, P. M.:
404 Response of intertidal populations to climate: effects of extreme events versus long term
405 change, *J. Exp. Mar. Biol. Ecol.*, 400, 132–144, 2011.
- 406 Whan, K., and Zwiers, F.: The impact of ENSO and the NAO on extreme winter precipitation in
407 North America in observations and regional climate models, *Clim. Dyn.*, 48, 1401–1411,
408 2017.



- 409 Wu, Z., and Lin, H.: Interdecadal variability of the ENSO–North Atlantic Oscillation connection
410 in boreal summer. *Q. J. Roy. Meteor. Soc.*, 138: 1668–1675, 2012.
- 411 Yun, X., Huang, B., Cheng, J., Xu, W., Qiao S., and Li, Q.: A new merge of global surface
412 temperature datasets since the start of the 20th century, *Earth Syst. Sci. Data*, 11, 1629–1643,
413 2019.
- 414



414 **Table 1.** Basic information about the nine wave-exposed intertidal locations surveyed for this
415 study.
416

Location code	Name of studied intertidal location (geographic coordinates)	Closest tide reference station (geographic coordinates)
L1	Glasgow Head (45.3203° N, 60.9592° W)	Canso (45.3500° N, 61.0000° W)
L2	Deming Island (45.2121° N, 61.1738° W)	Whitehead (45.2333° N, 61.1833° W)
L3	Tor Bay Provincial Park (45.1823° N, 61.3553° W)	Larry's River (45.2167° N, 61.3833° W)
L4	Barachois Head (45.0890° N, 61.6933° W)	Port Bickerton (45.1000° N, 61.7333° W)
L5	Sober Island (44.8223° N, 62.4573° W)	Port Bickerton (45.1000° N, 61.7333° W)
L6	Duck Reef (44.4913° N, 63.5270° W)	Sambro (44.4833° N, 63.6000° W)
L7	Western Head (43.9896° N, 64.6607° W)	Liverpool (44.0500° N, 64.7167° W)
L8	West Point (43.6533° N, 65.1309° W)	Lockport (43.7000° N, 65.1167° W)
L9	Baccaro Point (43.4496° N, 65.4697° W)	Ingomar (43.5667° N, 65.3333° W)

417

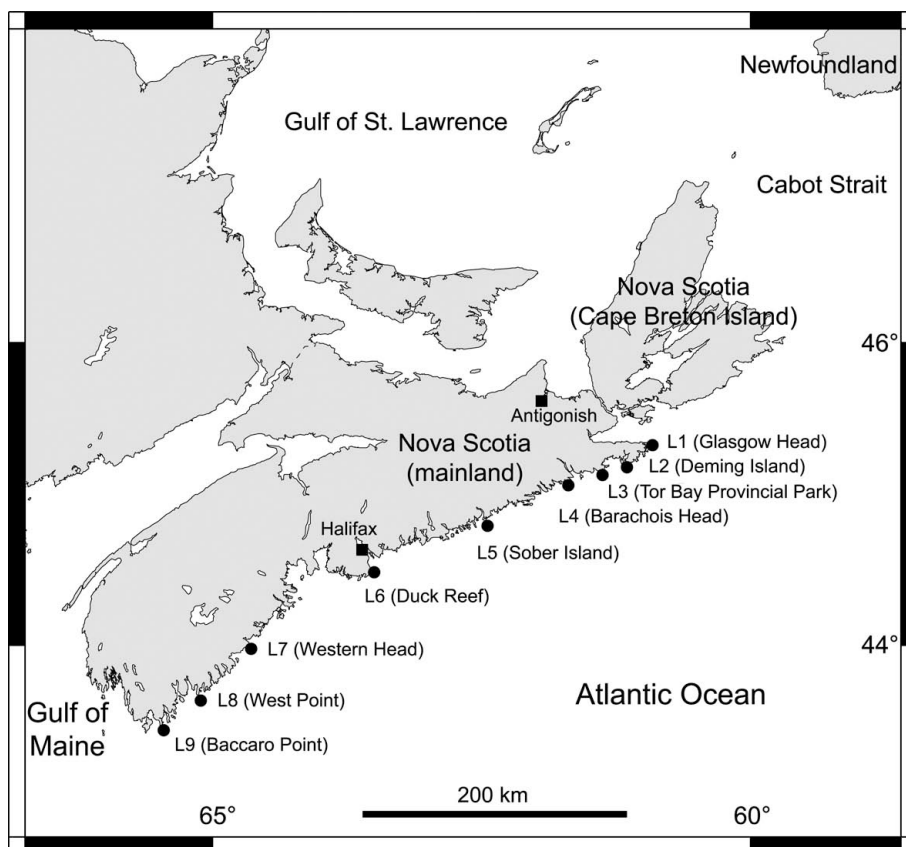


417 **Table 2.** Summary values of daily MaxT, MinT, and SST (°C) for the nine wave-exposed
 418 intertidal locations (L1 to L9, from north to south) surveyed between 2014 and 2019 along the
 419 Atlantic Canadian coast (see Methods for details on how each row of values was determined).

420

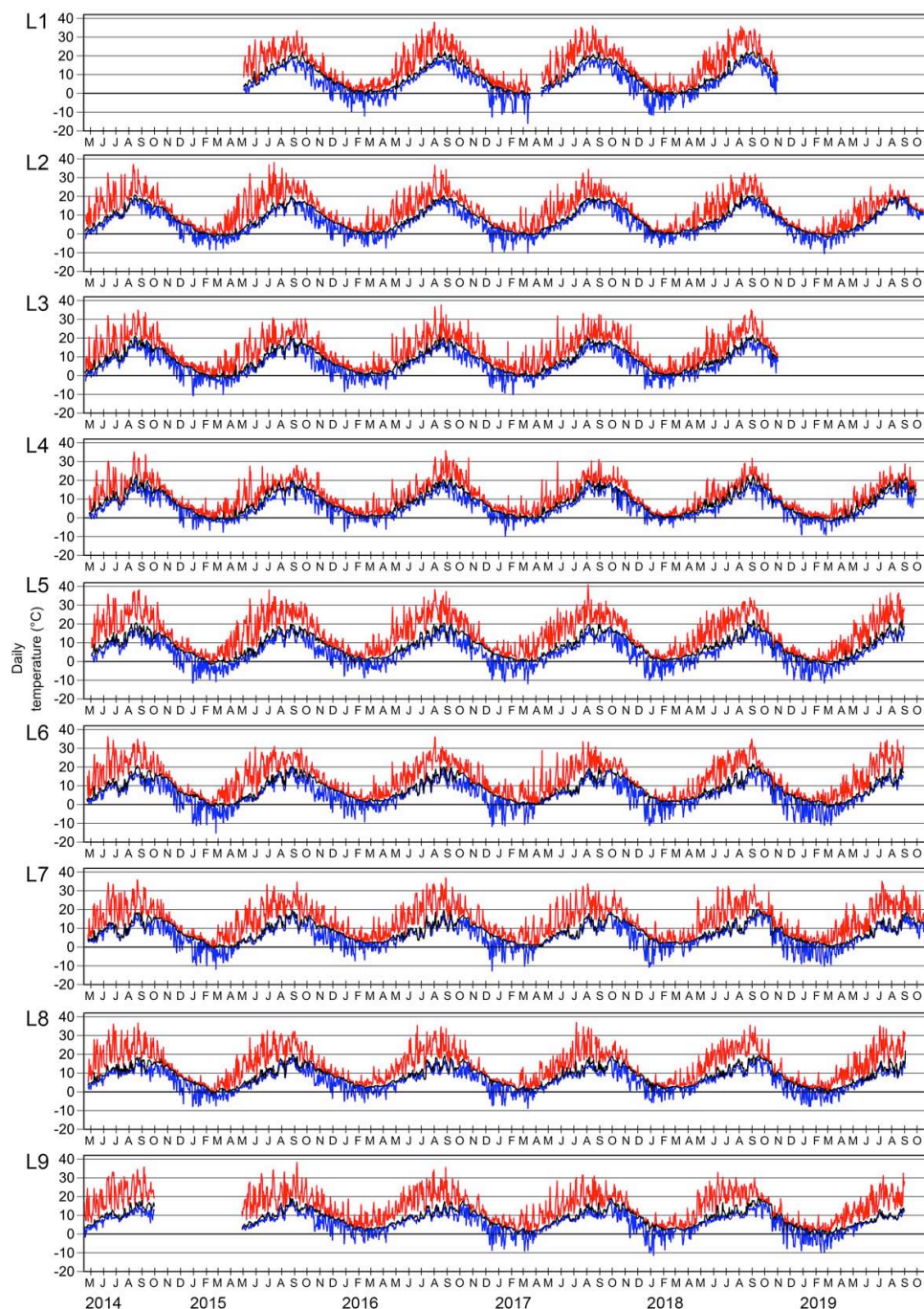
	L1	L2	L3	L4	L5	L6	L7	L8	L9
Highest daily MaxT	38.1	38.3	37.9	36.1	41.2	36.5	37.1	37.2	38.5
Lowest daily MinT	-16.3	-10.8	-11.0	-10.0	-12.2	-15.5	-13.0	-9.1	-11.6
Highest temperature range	54.4	49.1	48.9	46.1	53.4	52.0	50.1	46.3	50.1
Summer mean MaxT	25.1	22.9	22.6	20.7	25.5	23.5	22.8	23.2	21.8
Winter mean MinT	-2.7	-1.4	-1.3	-0.4	-2.2	-1.2	-0.3	0.02	0.2
Highest daily SST	22.5	21.5	21.8	22.8	22.2	21.9	20.3	22.1	20.0
Lowest daily SST	-1.7	-1.7	-1.4	-1.8	-1.8	-1.8	-0.9	-1.7	-1.7
Highest SST range	24.2	23.2	23.2	24.6	24.0	23.7	21.1	23.7	21.7
Summer mean SST	17.5	16.4	16.1	16.1	15.8	15.2	13.3	14.2	13.2
Winter mean SST	0.8	1.0	1.3	1.3	1.6	2.2	2.7	2.8	3.0

421



421
422
423
424
425

Figure 1. Map indicating the position of the nine wave-exposed intertidal locations surveyed along the Atlantic coast of mainland Nova Scotia, Canada.



425

426

427

Figure 2. Daily MaxT (red line), MinT (blue line), and SST (black line) at the nine intertidal locations (L1 to L9, from north to south) surveyed between April 2014 and October 2019.